

SUPPLEMENTAL MATERIALS

Calcification in human intracranial aneurysms is highly prevalent and displays both atherosclerotic and non-atherosclerotic types

Piyusha S. Gade¹, MS; Riikka Tulamo², MD, PhD; Keewon Lee, PhD¹; Fernando Mut³, PhD; Eliisa Ollikainen, MD, PhD^{5,9}; Chih-Yuan Chuang⁹, MS; Bong Jae Chung⁴, PhD; Mika Niemelä⁵, MD, PhD; Behnam Rezaei Jahromi⁵, MD, PhD; Khaled Aziz⁶, MD; Alexander Yu⁶, MD; Fady T. Charbel⁷, MD; Sepideh Amin-Hanjani⁷, MD; Juhana Frösen⁸, MD, PhD; Juan Cebra³, PhD; Anne M. Robertson^{1,9}, PhD

¹Department of Bioengineering, University of Pittsburgh, PA, USA

²Department of Vascular surgery, Helsinki University Hospital and University of Helsinki, Helsinki, Finland

³Department of Bioengineering, George Mason University, Fairfax, VA, USA

⁴Department of Mathematical Sciences, Montclair State University, Montclair, NJ, USA

⁵Department of Neurosurgery, Helsinki University Hospital and University of Helsinki, Helsinki, Finland

⁶Department of Neurosurgery, Allegheny General Hospital, Pittsburgh, PA, USA

⁷Department of Neurosurgery, University of Illinois at Chicago, Chicago, IL, USA

⁸Department of Neurosurgery, Kuopio University Hospital, Kuopio, Finland

⁹Department of Mechanical Engineering and Materials Science, University of Pittsburgh, PA, USA

Materials and Methods

Histological and Immunofluorescence Analysis

Samples were dehydrated in 30% sucrose solution at 4°C for 24 h. Tissue sections were embedded in optimal cutting temperature compound (Sakura Finetek, Torrance, CA, USA), frozen at -80°C overnight, and cryosectioned to 8µm thickness. This was followed by staining sections with H&E, Oil Red-O and Alizarin Red to stain for cell nuclei, lipids and calcification respectively.

Neutral lipid and free cholesterol staining

Tissue cryosections (8-µm thick) were fixed with 4% paraformaldehyde (PFA) for 1 h at 4°C and rinsed twice with PBS. For neutral lipid staining, BODIPY 493/503 (D3922, Thermofisher Scientific, Waltham, MA) was dissolved in dimethyl sulfoxide (DMSO) (D4540, Sigma-Aldrich, St. Louis, MO) at a concentration of 1 mg/ml and diluted to 1:500 with PBS. Tissue sections were stained with 100 µl of the BODIPY working solution, incubated for 30 min at 37°C in the dark, and rinsed twice with PBS. For free cholesterol staining, filipin (F9765, Sigma-Aldrich) was dissolved in DMSO at a concentration of 25 mg/ml and diluted to 1:500 with PBS. Tissue sections were stained with 100 µl of the filipin working solution, incubated for 2 h at room temperature in the dark, and rinsed twice with PBS. Stained slides were viewed using an inverted microscope with two fluorescence filters: green (for BODIPY, excitation = 450-510 nm) and blue (for filipin, excitation = 340-380 nm). Tissue slides without the staining reagents were used as negative controls. Human cerebral aneurysm tissue that presented with lipid pools on micro-CT images was used for positive controls.

Leukocyte and macrophage staining

Both leukocytes and macrophages were examined using immunofluorescence staining. Tissue cryosections (8-µm thick) were fixed with 4% PFA for 15 min at room temperature (RT). Tissue sections on slides were blocked with 3% normal goat serum (NGS) (Sigma-Aldrich) and 3% normal horse serum (Vector Laboratories) in buffer solution (3% bovine serum albumin in PBS) for 20 min at RT. incubated with primary antibodies in buffer solution for 30 min at RT, and rinsed with PBS, followed with the corresponding secondary antibodies in buffer solution at RT. For leukocyte staining, mouse anti-CD45 (clone 2B11 PD7/26, 1:100; Dako, Glostrup, Denmark) was used as a primary antibody, followed by Alexa Fluor 546 goat anti-mouse IgG (1:100, Invitrogen, Carlsbad, CA) as a secondary antibody. For macrophage staining, mouse anti-CD68 (clone EBM11, Dako) was used as a primary antibody, followed by Alexa Fluor 488 goat anti-mouse IgG (1:100, Invitrogen) as a secondary antibody. Nuclei were counterstained with 4',6-diamidino-2-phenylindole (DAPI) (Life Technologies, Carlsbad, CA). Tissue slides without primary antibodies were used as negative controls. Human tonsil was used for positive controls.

Calcification staining in histological sections

Micro-calcification was detected using a bisphosphonate-conjugated, near-infrared fluorescent imaging agent, OsteoSense 680 EX (PerkinElmer, Waltham, MA) as described previously¹. OsteoSense 680 EX was dissolved in 1.2 ml of PBS and applied to explanted samples for 2 h at room temperature. Samples were rinsed with PBS, fixed in 10% formalin for 1 h at 4°C, and dehydrated in 30% sucrose solution at 4°C for 24 h. Tissue sections were embedded in optimal cutting temperature compound, frozen at -80°C for 2 h, and cryosectioned to 8-µm thickness. Tissue slides were rinsed twice with PBS, mounted with fluorescence mounting medium, and viewed using an inverted microscope with the Cy5 filter (excitation = 630-680 nm). Calcified cerebral vessels were used as positive controls.

Calcification and collagen imaging in intact sample

Simultaneous imaging of collagen and calcification was performed using two photon microscopy as previously described¹. Briefly, the entire tissue sample was fixed in 4% PFA for 24h. This was followed by rinsing the sample with PBS. Sample was then incubated in OsteoSense 680EX (diluted 1:50) for 24h. This was followed by rinsing the sample with PBS and imaging with an Olympus two photon microscope (FV 1000, Tokyo, Japan) using the following settings: 1.12NA 259 MPE water immersion lens and 25X objective: 800nm excitation wavelength, dwell time of 8µs/pixel, a scan pixel count of 1024 X 1024 and laser intensity of 7%. Second harmonic signal from collagen was collected using a 350 – 450 nm filter and calcification signal using the fluorescent calcium tracer emission in the 665 – 735 nm channel.

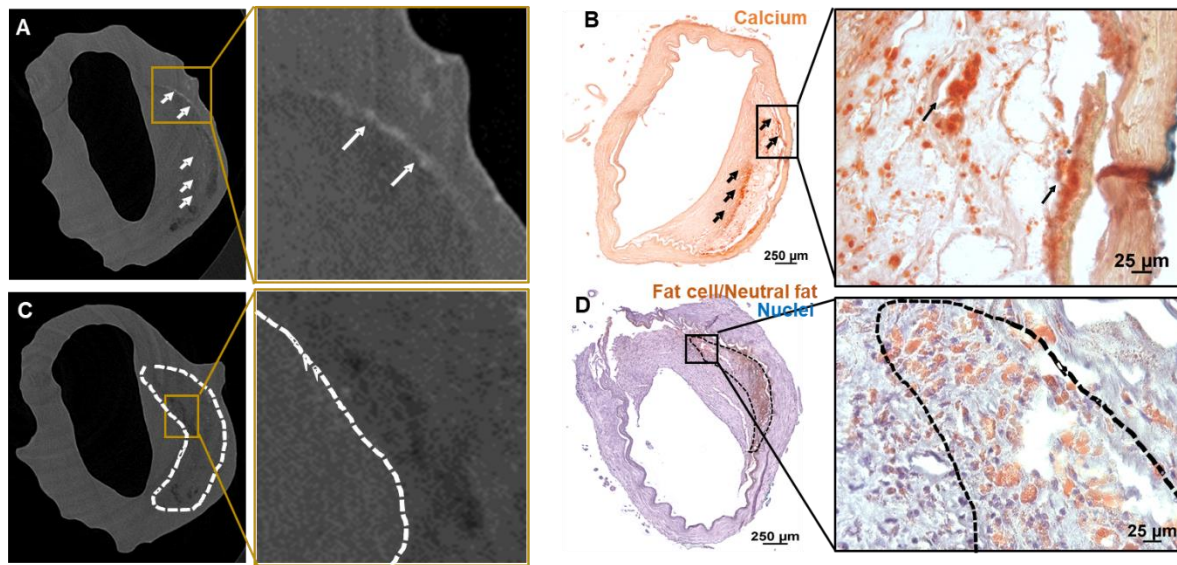
Lipid pool and calcification identification using micro-CT scanning in intact samples

Lipid pools and calcification manifest as regions with distinct peak intensity levels in micro-CT scanning of intact specimens. In the micro-CT images, lipid pools were identified as regions of low intensity (<30) with distinct morphological patterns. Samples were scored for presence or absence of lipid pools using these two criteria. Calcified regions presented with high grayscale values (220-255) in normalized images where 0 represents black and 255 represents white. Calcification was then segmented using either manual thresholding or an automatic multilevel Otsu segmentation technique, followed by region growing that joins connected components using an intensity-based approach.

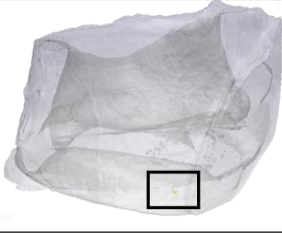
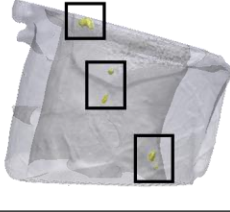


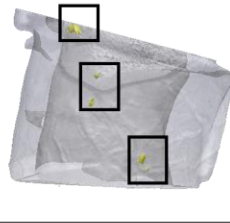

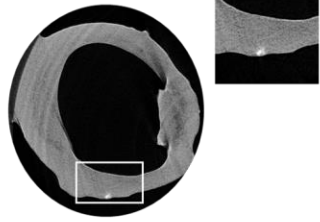
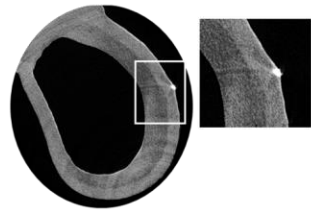
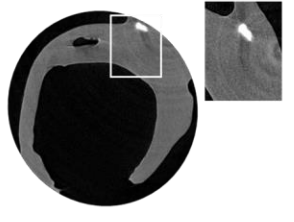
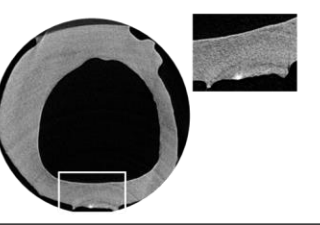
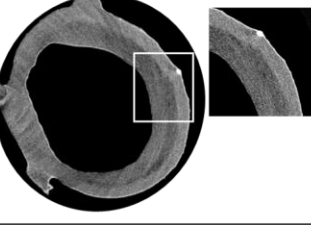
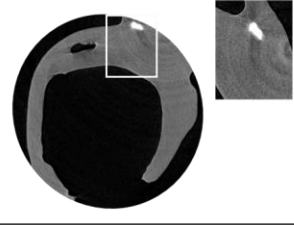
In order to verify specificity, we compared grey levels of calcification and lipid pools with their respective histological sections using Alizarin Red and Oil Red O as outlined above (Supplemental Figure I). False positives by hemorrhage or capillaries were ruled out by consideration of greyscale, morphology and size. In particular, hemorrhage regions have a greyscale value similar to that of tissue which lies in the 50 – 80 greyscale regime². Capillaries, if filled with blood, also appear at a similar intensity to that of tissue, thereby distinct from lipid pools and calcification. Additionally, capillaries are morphologically different (circular vs elliptical/irregular shaped) from lipid pools and have smaller diameters (5 – 10µm) when compared with the smallest size of lipid pools identified (20µm).

IA samples in our study were sourced from three sites - Alleghany General Hospital (AGH) (Pittsburgh, PA, USA), University of Illinois at Chicago (UIC) (Chicago, IL, USA), and Helsinki University Hospital (HUH) (Helsinki, Finland). Due to differences in site specific protocols (Finland versus U.S.) as well as differences in plans for further analysis (SEM versus classical histology), three different fixatives were used. Additional studies were performed to determine the role, if any, of each of the fixation methods on micro-CT results. Segments of cerebral artery were scanned before and after fixation for each fixative. Qualitatively there was no visual difference in terms of presence, location or morphology of calcification and lipid pools in micro-CT images as a result of fixation (Supplemental Figure II). Additionally, there was no differences in the relative attenuation levels of calcification and lipid pools due to fixation method, (Supplemental Figure II) with calcification remaining in the 220-250 regime and lipid pools and tissue in the < 30 and 50 – 80 respectively. Furthermore, the calcification volume pre and post-fixation were evaluated (using same fixation as for the aneurysm samples, Material and Methods of main text) and found to differ by less than 3% (Supplemental Table I).

Supplemental Figures



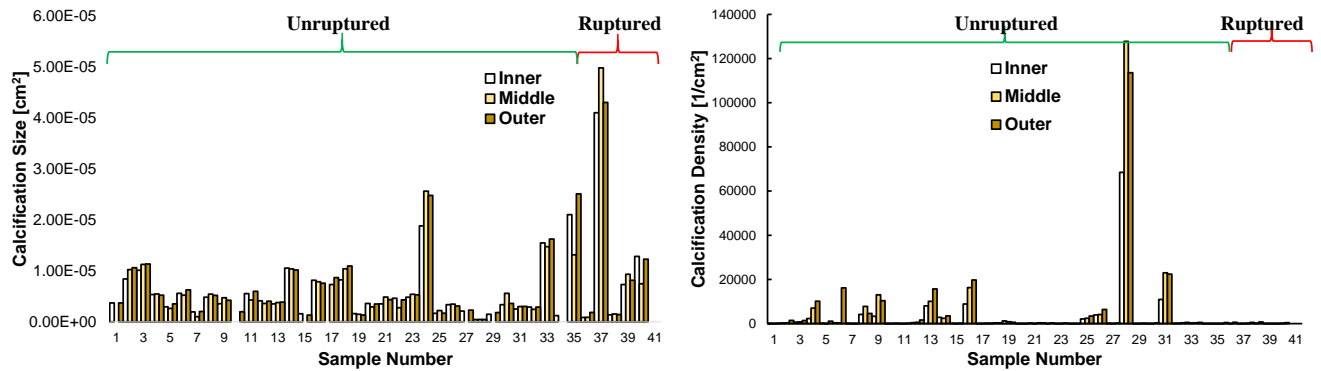
Supplemental Figure I: Verification of regions of calcification and lipid pools in control sample of a fresh cerebral artery identified under micro-CT (A) Cross sections from high resolution micro-CT image of fresh cerebral artery imaged at 2 μm resolution. White arrows point to micro-calcifications identified in micro-CT. (B) Alizarin Red staining confirming micro-calcifications (black arrows) as seen in micro-CT with high grayscale values (220-255) on a normalized scale. (C) Lipid pool (white dashed line) visible as low grayscale value in micro-CT image (< 30). (D) Oil Red O staining identifying neutral lipids (concentrated within black dashed line) in same sample. Nuclei were counterstained with hematoxylin.

A	Formalin	Glutaraldehyde	Paraformaldehyde
Pre Fixation			
Post Fixation			
B	Formalin	Glutaraldehyde	Paraformaldehyde
Pre Fixation			
Post Fixation			

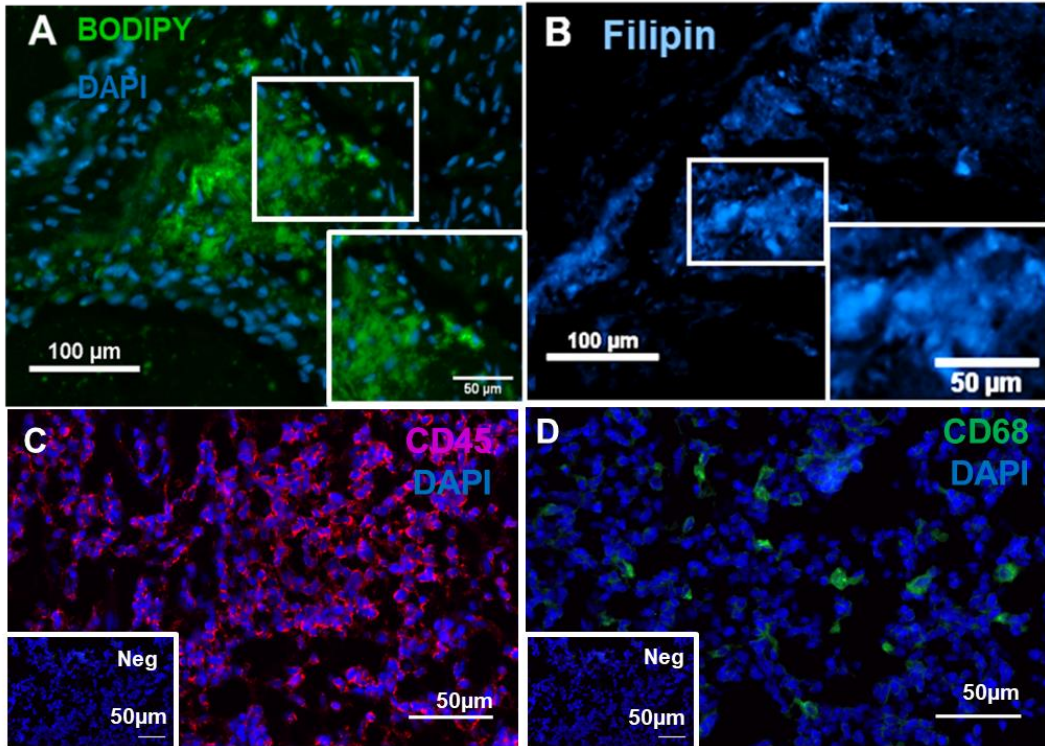
Supplemental Figure II: Comparison of cerebral vessels pre and post-fixation with micro-CT scanning. (A) 3D reconstruction of micro-CT scanned vessels, pre and post fixation in three different fixatives – 10% formalin, 3% glutaraldehyde and 4% paraformaldehyde. Calcification seen in yellow. (B) Cross section micro-CT images of (A) showing calcification in white.

Supplemental Table I: Calcification volume pre and post fixation in three fixatives - 10% formalin, 3% glutaraldehyde and 4% paraformaldehyde

	Pre Fixation Calcification Volume [mm ³]	Post Fixation Calcification Volume [mm ³]	% Difference pre and post fixation
Formalin	0.000583	0.000585	0.343
Glutaraldehyde	0.0023	0.00236	2.608
Paraformaldehyde	0.0012	0.00122	1.667



Supplemental figure III: (A) Calcification size and (B) density both increase with distance from the lumen with highest density and largest size of calcification located in the outer third of the wall.



Supplemental figure IV: Positive controls for immunofluorescent staining in a human cerebral aneurysm(A-B) and human tonsil (C-D) sample. Free cholesterol and neutral lipids are stained with (A) BODIPY and (B) Filipin respectively. Inflammatory cells are stained using (C) CD45, a pan leukocyte marker and, (D) CD68, macrophage marker. Nuclei are counterstained using DAPI. Negative controls for CD45 and CD68 (primary antibody omitted) are shown as insets in C, D.

Major Resources Tables

Antibodies

Name	Target antigen	Vendor or Source	Catalog #	Working concentration	Lot # (preferred but not required)
BODIPY 493/503	Neutral lipid	ThermoFisher Scientific,	D3922	2 µg/ml	1973430
Filipin	Free cholesterol	Sigma-Aldrich	F9765-25MG	50 µg/ml	N/A
CD45	CD45 (human)	Dako	GA75161-2	3.75 µg/ml	N/A
CD68	CD68 (human)	Dako	GA60961-2	2.37 µg/ml	N/A

References for Supplemental Material

1. Gade P, Robertson A, Chuang C. Multiphoton Imaging of Collagen, Elastin and Calcification in Intact Soft Tissue Samples. *Curr Protoc Cytom.* 2017.
2. Wintermark M, Jawadi SS, Rapp JH, Tihan T, Tong E, Glidden D V, Abedin S, Schaeffer S, Acevedo-Bolton G, Boudignon B, Orwoll B, Pan X, Saloner D. High-resolution CT imaging of carotid artery atherosclerotic plaques. *Am J Neuroradiol.* 2008;29:875-882.